

PRECISE PHASE NOISE MEASUREMENTS OF OSCILLATORS  
AND OTHER DEVICES FROM APPROXIMATELY 0.1 MHz TO 100 GHz,

Fred L. Walls  
Time and Frequency Division  
National Bureau of Standards  
Boulder, Colorado 80303

ABSTRACT

In this talk the commonly used measures of phase noise are briefly defined and their relationships explained. Techniques for making precise measurements of phase noise in oscillators, multipliers, dividers, amplifiers, and other components are discussed. Particular attention is given to methods of calibration which permit accuracies of 1 dB or better to be achieved. Common pitfalls to avoid are also covered. It is shown that the two oscillator approach is the most versatile of these techniques offering simultaneously both the lowest noise floor and the widest bandwidths. Phase noise floors (**precisions**) in **excess** of -170 dB relative to 1 **radian**<sup>2</sup> per hertz are achievable for carrier frequencies from well below 0.1 MHz to beyond 100 GHz range. The disadvantage for precise source measurements is the need for a reference source of comparable or better performance. This limitation does not apply to the measurement of amplifiers, multipliers, dividers, etc. Other techniques avoid this requirement by using a delay line or cavity to generate a pseudo reference generally with some sacrifice in noise floor near the carrier and bandwidth limitations. **Analogues** of these techniques are used for carrier frequencies from a few Hz to 10<sup>15</sup> Hz.

I. INTRODUCTION

The output of an oscillator can be expressed as

$$V(t) = [V_0 + \epsilon(t)] \sin(2\pi\nu_0 t + \phi(t)) \quad (1)$$

where  $V_0$  is the nominal peak output voltage, and  $\nu_0$  is the nominal frequency of the oscillator. The time variations of amplitude have been incorporated into  $a(t)$  and the time variations of the actual frequency,

Work of the U.S. Government; not subject to copyright.

$v(t)$ , have been incorporated into  $\phi(t)$ . The actual frequency can now be written as

$$v(t) = \nu_0 + \frac{d[\phi(t)]}{2\pi dt} \quad (2)$$

The fractional frequency deviation is defined as

$$y(t) = \frac{v(t) - \nu_0}{\nu_0} = \frac{d[\phi(t)]}{2\pi\nu_0 dt} \quad (3)$$

Power spectral analysis of the output signal  $V(t)$  combines the power in the carrier  $\nu_0$  with the power in  $\epsilon(t)$  and  $\phi(t)$  and therefore is not a good method to characterize  $\epsilon(t)$  or  $\phi(t)$ .

Since in many precision sources understanding the variations in  $\phi(t)$  or  $y(t)$  are of primary importance, we will confine the following discussion to frequency-domain measures of  $y(t)$ , neglecting  $\epsilon(t)$  except in cases where it sets limits on the measurement of  $y(t)$ . The amplitude **fluctuations**,  $\epsilon(t)$ , can be reduced using limiters whereas  $\phi(t)$  can be reduced in some cases by the use of narrow band filters.

Spectral (Fourier) analysis of  $y(t)$  is often expressed in terms of  $S_\phi(f)$ , the spectral density of phase fluctuations in units of radians squared per Hz bandwidth at Fourier frequency ( $f$ ) from the carrier  $\nu_0$ , or  $S_{yy}(f)$ , the spectral density of fractional frequency fluctuations in a 1 Hz bandwidth at Fourier frequency  $f$  from the carrier  $\nu_0$  [1]. These are related as

$$S_\phi(f) = \frac{\nu_0^2}{f^2} S_{yy}(f) \text{ rad}^2/\text{Hz} \quad 0 < f < \infty \quad (4)$$

$S_\phi(f)$  can also be intuitively understood as

$$S_\phi(f) = \frac{\Delta\phi^2(f)}{\text{BW}}, \quad (5)$$

where  $\Delta\phi$  is measured at Fourier frequency  $f$  from the carrier in a bandwidth BW. It should be noted that these are single-sided spectral density measures containing the phase or frequency fluctuations from both sides of the carrier.

Other measures sometimes encountered are  $\mathcal{L}(f)$ , dBC/Hz, and  $S_{yy}(f)$ . These are related by [1,2]

$$\begin{aligned} S_{yy}(f) &= \nu_0^2 S_y(f) \text{ Hz}^2/\text{Hz} \\ \mathcal{L}(f) &= (1/2) S_\phi(f) \quad f_1 < |f| < \infty \end{aligned} \quad (6)$$

$$\text{for } \int_{f_1}^{\infty} S_{\phi}(f) df < 1 \text{ rad}^2$$

$$\text{dBc/Hz} = 10 \log_{10} \mathcal{L}(f)$$

$\mathcal{L}(f)$  and dBc/Hz are single sideband measures of phase noise which are not defined for large phase excursions and are therefore measurement system dependent. Because of this an IEEE subcommittee on frequency stability recommended the use of  $S_{\phi}(f)$  which is well defined independent of the phase excursion [1]. This distinction is becoming increasingly important as users require the specification of phase noise near the carrier where the phase excursions are large compared to 1 radian. Single sideband phase noise can be specified as  $(\frac{1}{2} S_{\phi}(f))$ .

#### MEASUREMENT OF $S_{\phi}(f)$ BETWEEN TWO OSCILLATORS

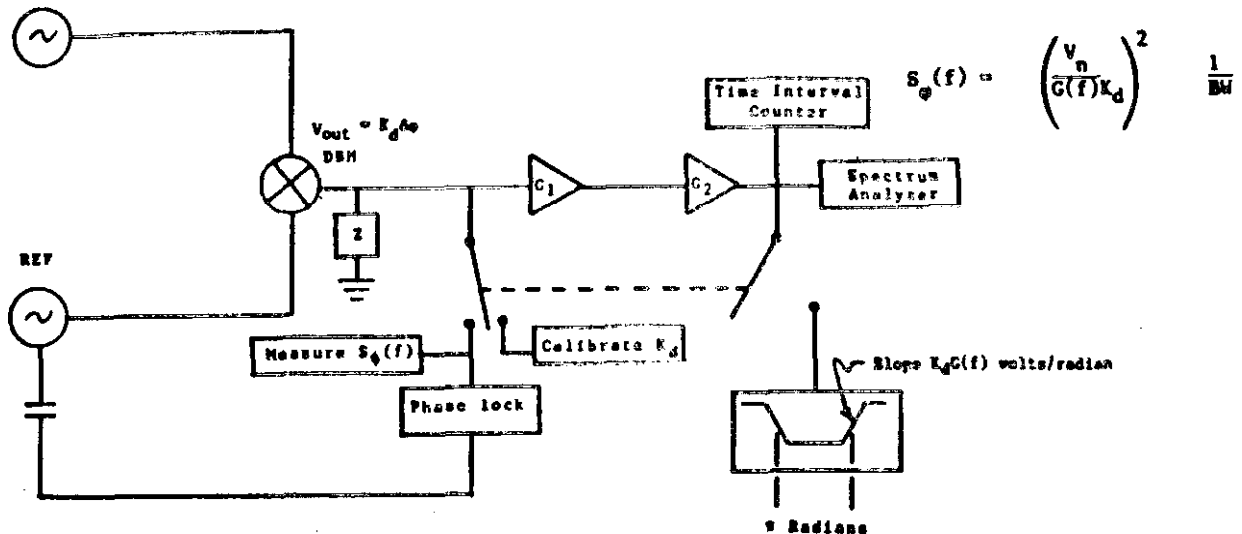


Figure 1. Precision phase measurement system using a spectrum analyzer. Calibration requires a recording device to measure the slope at the zero crossing. The accuracy is better than 0.2 dB from dc to 0.1  $\nu_0$  Fourier frequency offset from the carrier  $\nu_0$ . Carrier frequencies from a few Hz to  $10^{10}$  Hz can be accommodated with this type of measurement system. [3]

The above measures provide the most powerful (and detailed) analysis for evaluating types and levels of fundamental noise and spectral density structure in precision oscillators and signal handling equipment as it allows one to examine individual Fourier components of residual phase (or frequency) modulation. On the other hand, this analysis is extremely detailed and one often needs an analysis of the long-term average performance, such as the Allan Variance [1].

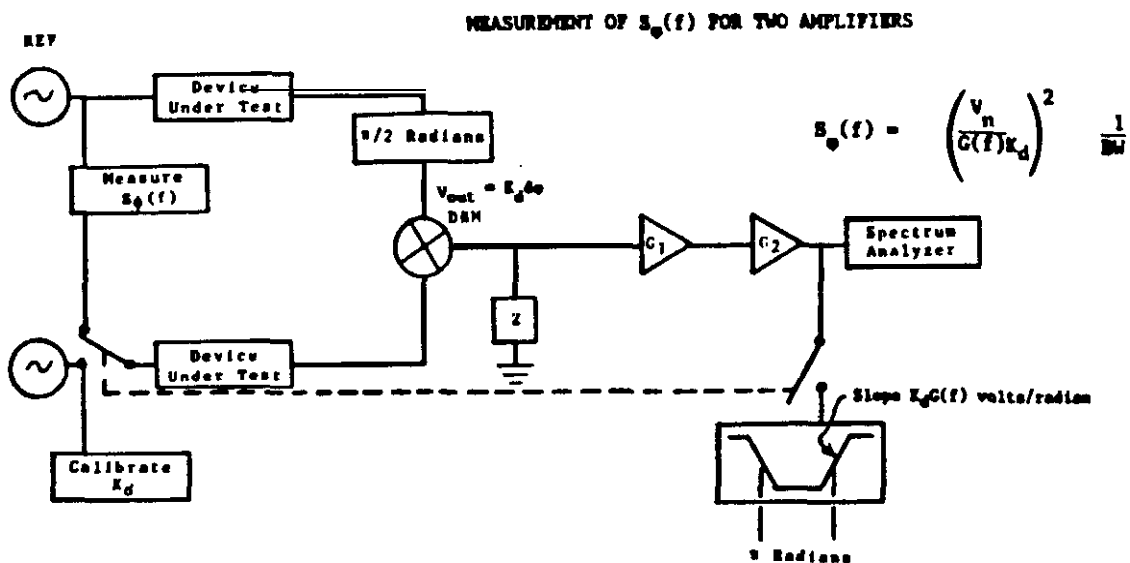


Figure 2. Precision phase measurement system featuring self calibration to 0.2 dB accuracy from dc to  $0.1 \nu_0$ . Fourier frequency offset from carrier. This system is suitable for measuring signal handling equipment, multipliers, dividers, frequency synthesizers, as well as passive components. [3]

## II. Methods of Measuring Phase Noise

### A. Two Oscillator Method

Figure 1 shows the block diagram for a typical scheme used to measure the phase noise of a precision source using a double balanced mixer and a reference source. Figure 2 illustrates a similar technique for measuring only the added phase noise of multipliers, dividers, amplifiers, and passive components. It is very important that the substitution oscillator be at the same drive level, impedance, and at the equivalent electrical length from the mixer as the signal coming from the reference oscillator. This is dramatically illustrated in Figure 3, discussed below. The output voltage of the mixer as a function of phase deviation,  $\Delta\phi$ , between the two inputs is nominally given by

$$V_{out} = K \cos \Delta\phi \quad (7)$$

Near quadrature this can be approximated by

$$V_{out} = K_d \delta\phi, \text{ where } \delta\phi \equiv \left[ \Delta\phi - \frac{2n-1}{2} \pi \right] < .1 \quad (8)$$

where  $n$  is the integer to make  $\delta\phi \approx 0$ . The phase to voltage conversion ratio sensitivity,  $K_d$ , is dependent on the frequency, the drive level, and impedance of both input signals, and the IF termination of the mixer [7].

The combined spectral density of phase noise of both input signals including the mixer and amplitude noise from the IF amplifiers is given by

$$S_{\phi}(f) = \left( \frac{V_n}{G(f)K_d} \right)^2 \frac{1}{S W} \quad (9)$$

where  $V_n$  is the RMS noise voltage at Fourier frequency  $f$  from the carrier measured after IF gain  $G(f)$  in a noise bandwidth  $BW$ . Obviously  $BW$  must be small compared to  $f$ . This is very important where  $S_{\phi}(f)$  is changing rapidly with  $f$ , e.g.,  $S_{\phi}(f)$  often varies as  $f^{-3}$  near the carrier. In Fig. 1, the output of the second amplifier following the mixer contains contributions from the phase noise of the oscillators, the mixers, and the post amplifiers for Fourier frequencies much larger than the phase-lock loop bandwidth. In Figure 2, the phase noise of the oscillator

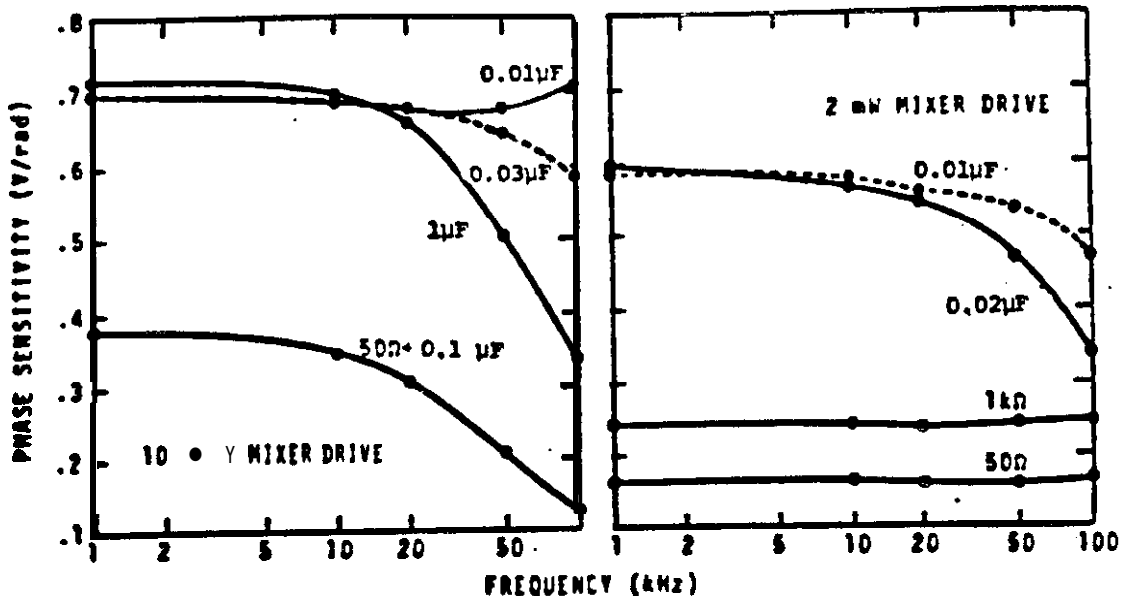


Figure 3. Double-balanced mixer phase sensitivity at 5 MHz as a function of Fourier frequency for various output terminations. The curves on the left were obtained with 10 mW drive while those on the right were obtained with 2 mW drive. The data demonstrate a clear choice between constant, but low sensitivity or much higher, but frequency dependent sensitivity. [3]

cancels out to a high degree (often more than 20 dB). Termination of the mixer IF port with 50 ohms maximizes the IF bandwidth, however, termination with reactive loads can reduce the mixer noise by ~ 6 dB, and increase  $K_d$  by 3 to 6 dB as shown in Fig. 3. [3] Accurate determination of  $K_d$  can be achieved by allowing the two oscillators to slowly beat and measuring the slope of the zero crossing in volts/radian with an oscilloscope or other recording device. For some applications the FFT often used to measure the noise voltage can be made to digitize the beat frequency waveform. The time axis is easily calibrated since one beat period equals  $2\pi$  radians. For some applications the digitizer in the spectrum analyzer can be used to measure both the beat period and the slope in volts/s at the zero crossing. The slope in volts/radian is then easily calculated with very high accuracy (0.1 dB). Estimates of  $K_d$  obtained from measurements of the peak to peak

output voltage sometimes introduce errors as large as 6 dB in  $S_{\phi}(f)$  even if the amplitude of the other harmonics is measured unless the phase relationship is also taken into account [3]. By comparing the level of an IF signal (a pure tone is best), on the spectrum analyzer used to measure  $V_n$  with the level recording device used to measure  $K_d$ , the accuracy of  $S_{\phi}(f)$  can be made independent of the accuracy of the spectrum analyzer voltage reference. The noise bandwidth of the spectrum analyzer also needs to be verified. If measurements need to be made at Fourier frequencies near or below the phase lock loop bandwidth, a probe signal can be injected inside the phase lock loop and the attenuation measured versus Fourier frequency. This provides the necessary correction factor for these phase noise measurements. Some care is necessary to assure that the spectrum analyzer is not saturated by spurious signals such as the line frequency and its multiples. Sometimes aliasing in the spectrum analyzer is a problem. Typical best performance is shown in Fig. 4. This measurement approach exceeds the performance of almost all available oscillators

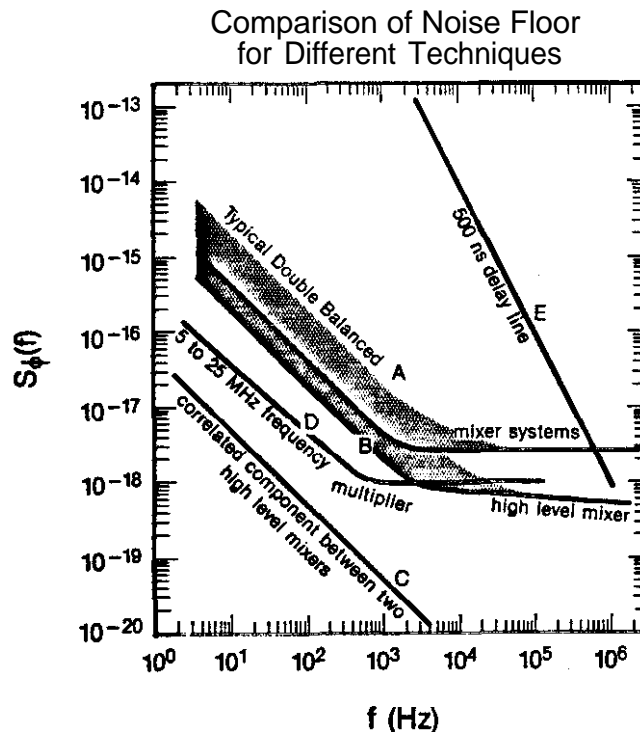


Figure 4.

- Curve A. The noise floor  $S_{\phi}(f)$  (resolution) of typical double balanced mixer systems (e.g. Fig. 1 and Fig. 2) at carrier frequencies from 0.1 to 700 MHz. Similar performance possible to 100 GHz. [4]
- Curve B. The noise floor,  $S_{\phi}(f)$ , for a high level mixer. [4]
- Curve C. The correlated component of  $S_{\phi}(f)$  between two channels using high level mixers. [4]
- Curve D. The equivalent noise floor  $S_{\phi}(f)$  of a 5 to 25 MHz frequency multiplier.
- Curve E. Approximate phase noise floor of figure 8 using a 500 ns delay line.

from below 0.1 MHz to **over** 100 GHz and is generally the technique of first choice because of its versatility and simplicity. Figures 10-13 give some examples. Using the above calibration procedure, phase noise measurements on signal sources can be made with an absolute accuracy better than 1 dB for signal sources. This accuracy is not always possible where the phase noise of the source exceeds that of the added noise of the components under test in Figure 2. The use of specialized mixers with multiple diodes per leg increases the phase to voltage conversion sensitivity,  $K_d$  and therefore reduces the contribution of IF amplifier noise [4] as shown in Fig. 4. Phase noise measurements can generally be made at Fourier frequencies from approximately dc to 1/2 the source frequency. The major difficulty being the **mixer** terminations and the difficulty of removing the source frequency from the output signal which would generally saturate the low noise amplifiers following the mixer.

Most double balanced mixers have a substantial non-linearity that can be exploited to make phase comparison between the reference source and odd multiples of the reference frequency. Some mixers even feature internal even harmonic generation. The measurement block diagram looks identical to that given in Figure 1, except the source under test is at an odd (even) harmonic of the reference source. This method is relatively efficient (as long as they fall within the bandwidth of the mixer) for multiples up to x5 although multiples as high as 25 have been observed. The noise floor is degraded by the amount of reduction in the phase sensitivity of the mixer. The phase noise of the reference source is also higher at the multiplied frequency as shown in II.F below.

#### B. Enhanced Performance Using Correlation Techniques

The resolution of the many systems can be greatly enhanced (typically 20 dB) using correlation techniques to separate the phase noise from the device under test from the noise in *the mixer* and IF amplifier [4].

For example consider the scheme illustrated in Figure 5. At the output of each double balanced mixer there is a signal which is proportional to the phase difference,  $\Delta\phi$ , between the two oscillators and a noise term,  $V_N$ , due to contributions from the mixer and amplifier. The voltages at the input of each **bandpass** filter are

$$V_1(\text{BP filter input}) = G_1 \Delta\phi(t) + C_1 V_{N1}(t), \quad (10)$$

$$V_2(\text{BP filter input}) = G_2 \Delta\phi(t) + C_2 V_{N2}(t),$$

where  $V_{N1}(t)$  and  $V_{N2}(t)$  are substantially **uncorrelated**. Each **bandpass** filter produces a narrow band noise function around its center frequency f:

$$V_1(\text{BP filter output}) = G_1 [S_\phi(f)]^{1/2} B_1^{1/2} \cos [2\pi ft + \phi(t)] \\ + C_1 [S_{V_{N1}}(f)]^{1/2} B_1^{1/2} \cos [2\pi ft + n_1(t)] \quad (11)$$

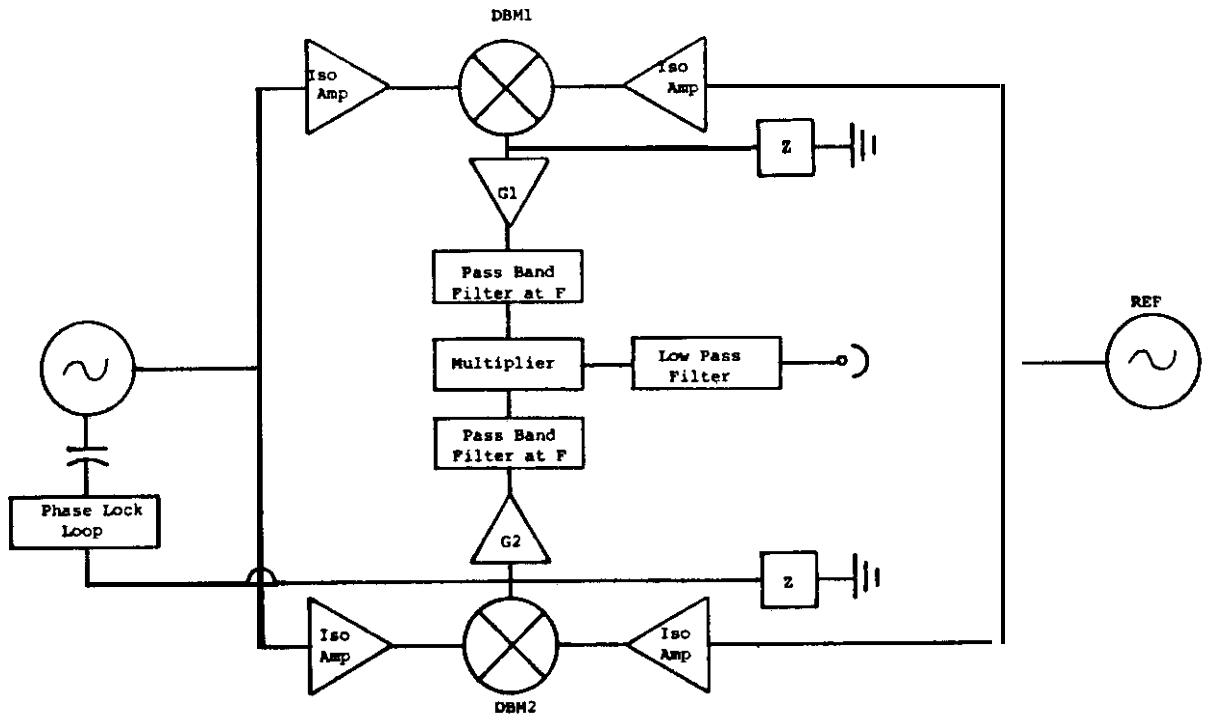


Figure 5. Correlation phase noise measurement system.

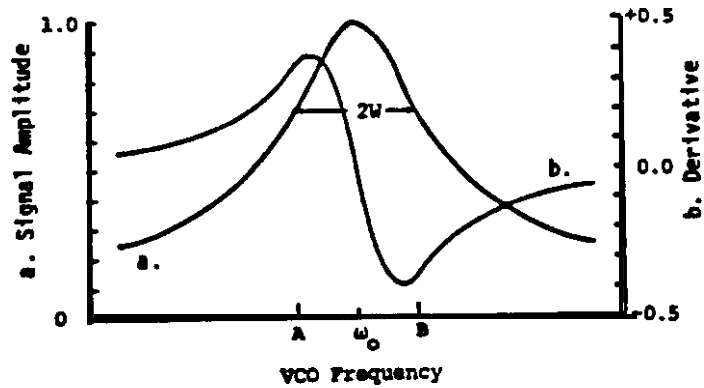


Figure 6. High-Q resonance used as a frequency discriminator. Note that the peak response is displaced from the center of the resonance by about the half bandwidth.



$$V_2(\text{BP filter output}) = G_2 [S_\phi(f)]^{1/2} B_2^{1/2} \cos [2\pi ft + \psi(t)] \\ + G_2 [S_{vN2}(f)]^{1/2} B_2^{1/2} \cos [2\pi ft + n_2(t)]$$

where  $B_1$  and  $B_2$  are the equivalent noise bandwidths of filters 1 and 2 respectively. Both channels are **bandpass** filtered in order to help eliminate aliasing and dynamic range problems. The phases  $\psi(t)$ ,  $n_1(t)$  and  $n_2(t)$  take on all values between 0 and  $2\pi$  with equal likelihood. They vary slowly compared to  $1/f$  and are substantially **uncorrelated**. When these two voltages are multiplied together and low pass filtered, only one term has finite average value. The output voltage is

$$V_{out}^2 \approx \frac{1}{2} G_1 G_2 S_\phi(f) B_1^{1/2} B_2^{1/2} + D_1 \langle \cos[2\psi(t)] \rangle \quad (12)$$

+  $D_2 \langle \cos[\psi(t) - n_2(t)] \rangle + D_3 \langle \cos[n_1(t) - n_2(t)] \rangle$  so that  $S_\phi(f)$  is given by

$$S_\phi(f) = \frac{(2)V_{out}^2}{G_1 G_2 \sqrt{B_1 B_2}} \quad (13)$$

For times long compared to  $B_1^{-1/2} B_2^{-1/2}$  the noise terms  $D_1$ ,  $D_2$  and  $D_3$  tend towards zero as  $1/\sqrt{t}$ . Limits in the reduction of these terms are usually associated with harmonics of 60 Hz pickup, dc offset drifts, and nonlinearities in the multiplier. Also if the isolation amplifiers have input current noise, they will pump current through the source resistance. The resulting noise voltage will appear coherently on both channels **and** can't be distinguished from real phase noise between the two oscillators. One half of the noise power appears in amplitude and one half in phase modulation.

Obviously the simple single frequency correlator used in this illustration can be replaced by a fast digital system which simultaneously computes the correlated phase noise for a large band of Fourier frequencies. Typical results show a reduction in noise floor of order 20 dB over the noise floor of a single channel (See Fig. 4). The great power of this technique is that it can be applied at any carrier frequency where one can obtain double balanced mixers. The primary limitations come from the bandwidth and nonlinearities in the cross correlator.

#### C. Reference Phase Modulation Method

Another method of determining  $S_\phi(f)$  **uses** phase modulation of the reference oscillator by a known amount. The ratio of the reference phase modulation to the rest of the spectrum then can be used for a relative calibration. This approach **can** be very useful for measurements which are repeated a great many times.

#### D. Frequency Discriminator Methods

It is sometimes convenient to use a high-Q resonance directly as a frequency discriminator as shown in Fig. 6. The oscillator can be tuned  $1/2$  linewidth ( $\nu_o/2Q$ ) away from line center yielding a detected signal of the form

$$V_{out} = G(f)k_d Q dy(f) [V + \epsilon(t)] . \quad (14)$$

Note that this approach mixes frequency fluctuations between the oscillator and reference resonance with the amplitude noise of the transmitted signal. By using amplitude control (e.g. by processing to normalize the data), one can reduce the effect of amplitude noise. [5] The measured noise at the detector is then related to the phase fluctuation of the reference resonance by

$$S_\phi(f) = \left[ \frac{\nu_o V_N}{f Q k_d G(f)} \right]^2 \frac{1}{BW} \quad f < \frac{\nu_o}{2Q} \quad (15)$$

This approach has the limitations that  $\Delta\nu$  must be small compared to the linewidth of the cavity, and removing the effect of residual amplitude noise is difficult; however, no reference source is needed.

Differential techniques can be used to measure the inherent frequency (phase) fluctuations of two high-Q resonators as shown in Fig. 7 [6]. The output voltage is of the form  $V_{out} = 2QK_d dy(f)$ . The phase noise spectrum of the resonators is then obtained using equation 4.

$$S_\phi(f) = \left[ \frac{\nu_o V_N}{2QfK_d G(f)} \right]^2 \frac{1}{BW} \quad f < \frac{\nu_o}{2Q} . \quad (16)$$

The phase noise in the **source** can cancel out by 20 to 40 dB depending on the similarity of resonate frequencies  $Q$ 's and the transmission properties of the two resonators. This approach was first used to demonstrate that the inherent frequency stability of precision quartz resonators **exceeds** the performance of most quartz crystal controlled oscillators [6].

If only one resonance is used, the output includes the phase fluctuations of both the source and the resonator. The calibration is accomplished by stepping the frequency of the source and measuring the output voltage, **ie**  $\Delta V = G(f)K^1(f) \Delta\nu_1$ . From this measurement the phase spectrum can be calculated as

$$S_\phi(f) = \frac{V_N^2}{K^1(f) f^2} \left( \frac{1}{BW} \right) . \quad (17)$$

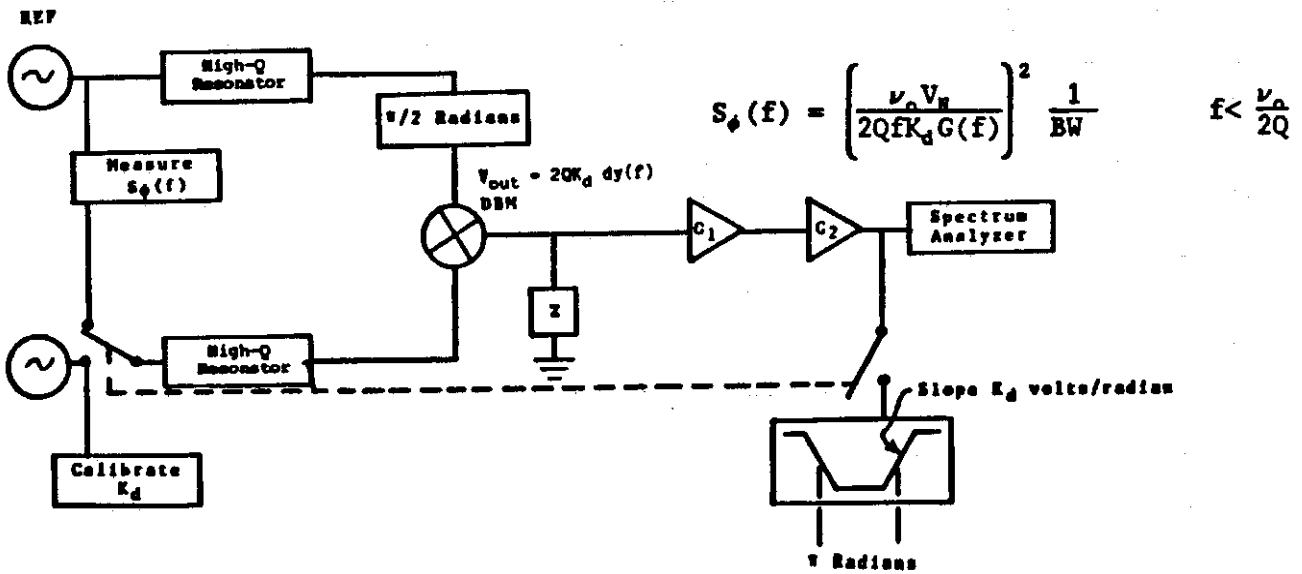


Figure 7. Differential frequency discriminator using a pair of high-Q resonators. In this approach the phase noise of the source tends to cancel out.

Figure 8A shows one method of implementing this approach at X-hand. The cavity has a loaded quality factor of order 25,000. Figure 8B shows the measured frequency discriminator curve. Note that  $K^1(f)$  is constant for  $f < \nu_o / (2Q)$  and decreases at values of  $f$  larger than the half bandwidth or the resonance as

$$K^1(f) \sim \frac{2Q/\nu_o}{1 + \left(\frac{2Qf}{\nu_o}\right)^2} \quad (18)$$

#### E. Delay Line Method

A still different approach uses a delay line to make a pseudo reference which is retarded relative to the incoming signal [7-10] as shown in Fig. 9.

The mixer output is of the form

$$V_{out} = 2\pi\tau_d K_d \nu_o dy \quad (19)$$

and the input phase noise is given by

$$S_{\phi}(f) = \left[ \frac{V_n}{2\pi f \tau_d G(f) K_d} \right]^2 \frac{1}{BW}, \quad f < \frac{1}{\tau_d} \quad (20)$$

This approach is often used at microwave frequencies when only one oscillator is available. However the ability to resolve phase noise close to the carrier depends on the delay time. For example if  $f = 1$  Hz and  $\tau_d = 500$  ns, then,  $(2\pi f\tau_d)^2 \sim 10^{-11}$ . For this example the noise floor is 110 dB higher at  $f = 1$  Hz than that of the two oscillator method decreasing as  $1/f^2$ . Recent advances make it possible to encode the rf signal on an optical signal which then can be transmitted down an optical fiber to achieve delays up to the order of  $10^{-3}$ s with some increase in the noise floor. The noise floor can be reduced by approximately 20 to 40 dB using the correlation techniques described above. [10] Note that the bandwidth is limited to less than  $\sim 1/\tau_d$ .

#### F. Multiplication/Division

The use of perfect frequency multipliers (or dividers) between the signal source and the double balanced mixer increases (decreases) the phase noise level [11] as

$$S_{\phi\nu_2}(f) = \left(\frac{\nu_2}{\nu_1}\right)^2 S_{\phi\nu_1}(f) . \quad (21)$$

This can be used to either increase **or** decrease the phase sensitivity of the mixer system. Figure 4 shows the noise of a specialized 5 to 25 MHz multiplier referred to the 5 MHz input. A potential problem with the use of the multiplier approach **comes from exceeding** the dynamic range of the mixer. Once the phase excursion,  $\Delta\phi$ , exceeds about 0.1 radian, **nonlinearities** start to become important and at  $A_4 \sim 1$  radian, the measurement is no longer valid [11].

#### ACKNOWLEDGEMENTS

The author is grateful to many colleagues, especially David W. **Allan**, James C. Bergquist, Andrea **DeMarchi**, David J. Glaze, James E. Gray, David A. Howe, Samuel R. Stein and Charles Stone for many fruitful discussions on this topic and to the Calibration Coordination Group for the funding to improve the accuracy and bandwidth of phase noise metrology.

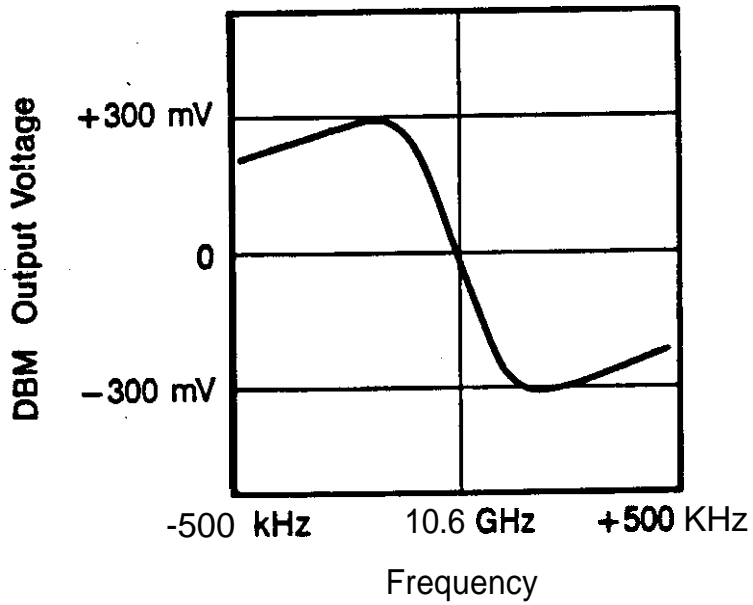
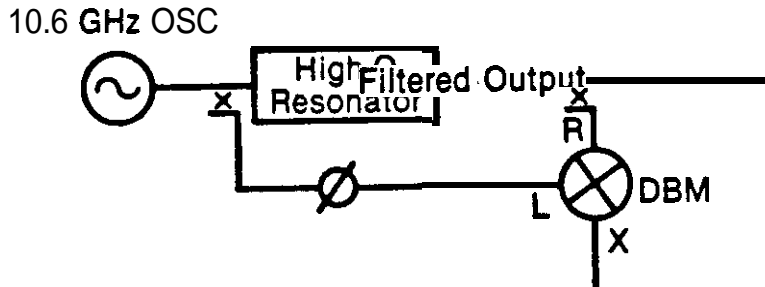


Figure 8. A. block diagram of a high Q resonator used as a frequency discriminator. B. Frequency discriminator curve for the scheme shown in A used at X-band with a cavity having a loaded quality factor of approximately 25,000.

MEASUREMENT OF  $S_{\phi}(f)$  USING A DELAY LINE

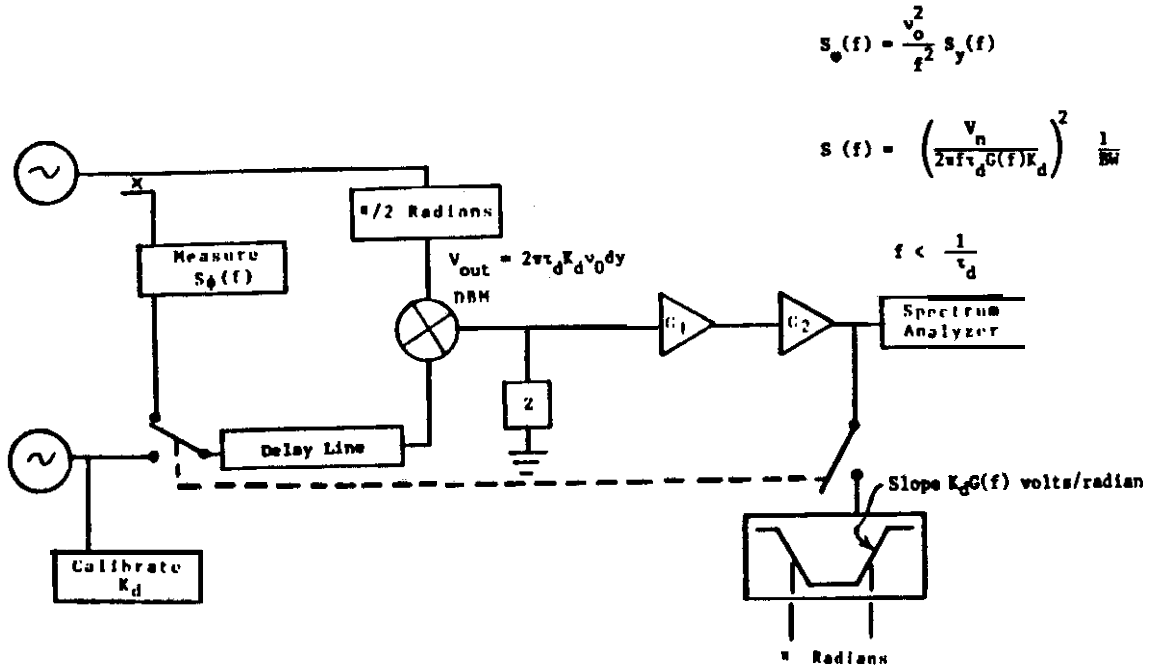


Figure 9. Delay line frequency discriminator.

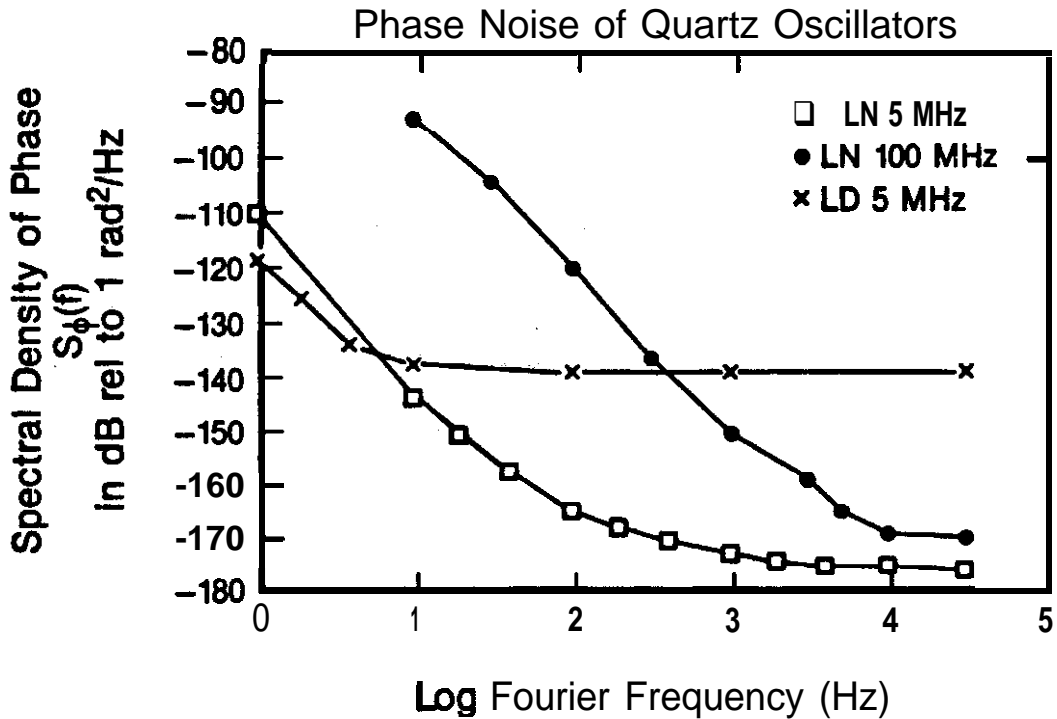


Figure 10. Phase noise performance of selected quartz oscillators.

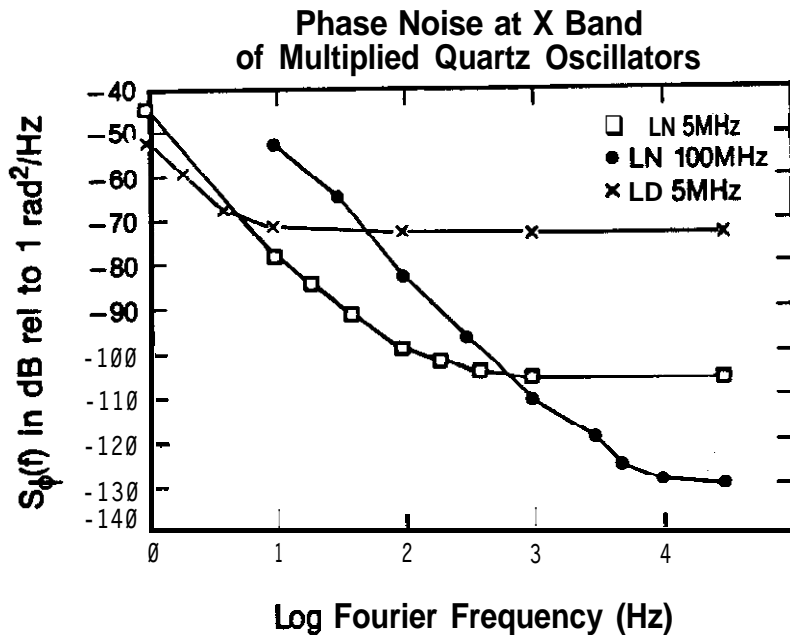


Figure 11. Phase noise of the oscillators of figure 10 if multiplied to X-band in a perfect frequency multiplier.

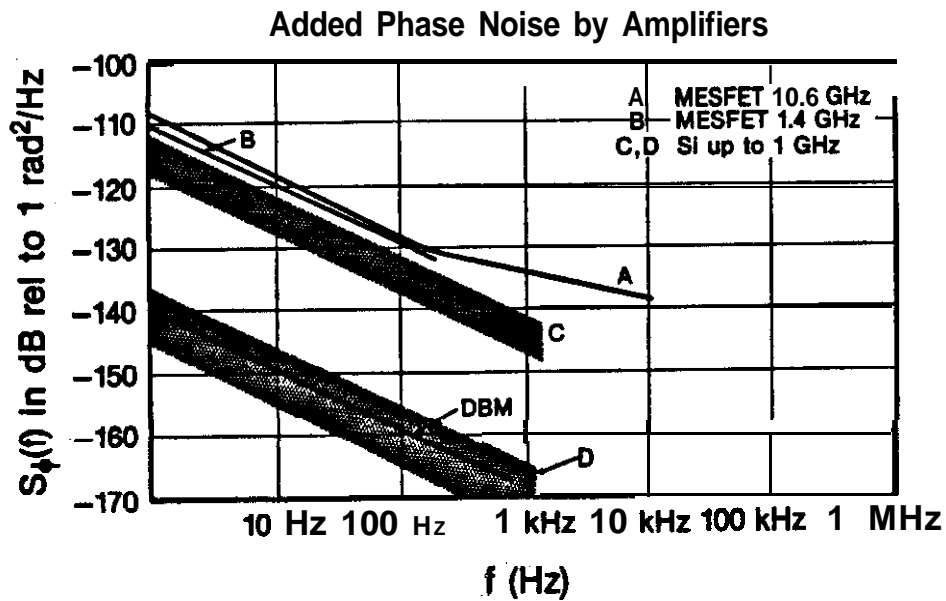


Figure 12. Curves A and B show the phase noise added by selected GaAs MESFET amplifiers. Curve C shows the phase noise added by a typical common emitter silicon bipolar transistor with a "good" rf bypass on the emitter lead. Curve D shows the typical performance of the same amplifier with a small unbypassed impedance (approximately  $1/\text{transconductance}$ ) in the emitter lead. The added phase noise is generally independent of frequency over a very large range.

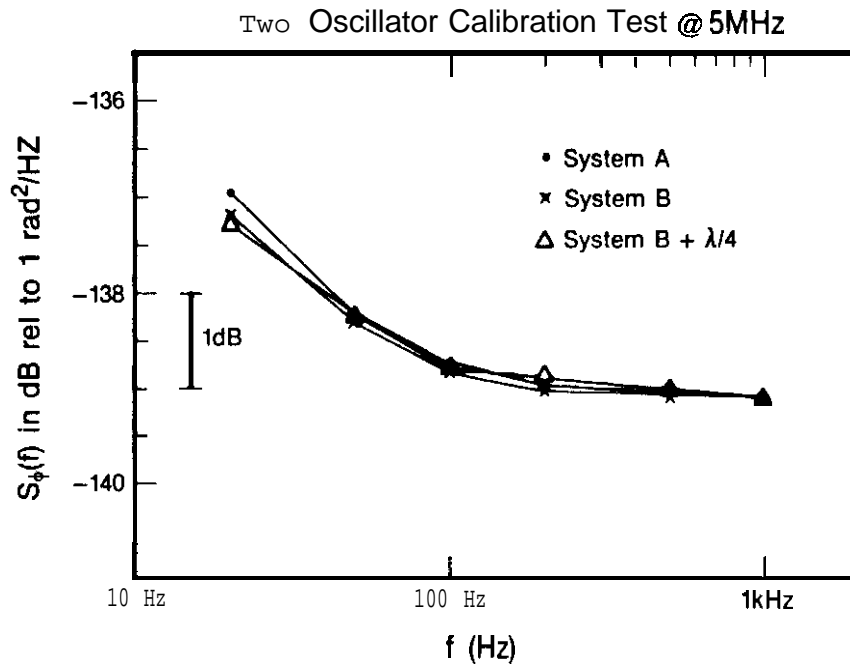


Figure 13. Demonstration of calibration accuracy for **two** oscillator concept of Fig. 1. The curve labeled System A shows the measured phase noise of a pair of 5 MHz oscillators using the test set shown in Fig. 1. The curve labeled System B shows the measured phase noise of the same pair of 5 MHz oscillators using a totally separate measurement system with the oscillators held in phase quadrature with the measurement test set of A. The curve labeled System B + X/4 shows the phase noise of the same pair of oscillators using the test set of B with X/4 cables between the oscillators and the measurement test set. The slope of the **zero** crossing of the beat was measured using the digitizer in the two different **FFT** spectrum analyzers. This measures  $K_d G(F)$  to about 1%. The agreement between the three curves is in the **worse** case  $\pm 0.15$  dB.

#### REFERENCES

1. Barnes, J.A., Chi, A.R., Cutler, L.S., Healey, D.J., Leeson, D.B., McGunigal, T.E., Mullen, Jr., J.A., Smith, W.L., Sydnor, R.L., Vessot, R.F.C., Winkler, G.M., Characterization of Frequency Stability, *Proc. IEEE Trans. on I & M* **20**, 1971, pp. 105-120.
2. Shoaf, J.H., Halford, D., and Risley, A.S., Frequency Stability Specifications and Measurement, NBS Technical Note 632, 1973. Document available from US Government printing office. Order SD at #C13.46:632.
3. Walls, F.L. and Stein, S.R., Accurate Measurements of Spectral Density of Phase Noise in Devices, *Proc. of 31st SFC*, 1977, pp. 335-343. (National Technical Information Service, Sills Building, 5825 Port Royal Road, Springfield, VA 22161).



4. Walls, F.L., Stein, S.R., Gray, J.E., and Glaze, D.J., Design Considerations in State-of-the-Art Signal **Processing** and Phase Noise Measurement Systems, **Proc.** 30th Ann. SFC, 1976, pp. 269-274. (National Technical Information Service, Sills Building, 5285 Port Royal Road, Springfield, VA 22161).
5. **Barger**, R.L., **Soren**, M.S., and Hall, J.L., Frequency Stabilization of a **cw** Dye Laser, **Appl. Phys. Lett.** 22, 1973, 573.
6. Walls, F.L. and Wainwright, A.E., Measurement of the Short-Term Stability of Quartz Crystal Resonators and the Implications for Crystal Oscillator Design and Applications, **IEEE Trans. on I & M** 24, 1975, pp. 15-20.
7. Risky, A.S., Shoaf, J.H., and Ashley, J.R., Frequency Stabilization of X-Band Sources for Use in Frequency Synthesis into the Infrared, **IEEE Trans. on I & M**, 23, 1974, pp. 187-195.
8. Ashley, J.R., Barley, T.A., and **Rast**, G.J., The Measurement of Noise in Microwave Transmitters, **IEEE Trans. on Microwave Theory and Techniques**, Special Issue on Low Noise Technology, (1977).
9. Lance, A.L., Seal, W.D., **Mendoza**, F.G., and Hudson, **N.W.**, Automating Phase Noise Measurements in the Frequency Domain, **Proc.** 31st Ann. **Symp.** on **Freq.** Control, 1977, pp. 347-358.
10. **Lance**, A.L. and Seal, W.D., Phase Noise and AM Noise Measurements in the Frequency Domain at Millimeter Wave Frequencies, from Infrared and Millimeter Waves, Ken Button Ed., Academic Press, NY 1985.
11. Walls, F.L. and **DeMarchi**, A., RF Spectrum of a Signal After Frequency Multiplication Measurement and Comparison with a Simple Calculation, **IEEE Trans. on I & M** 24, 1975, pp. 210-217.